AIAA 2002–0243

Hybrid Wing Design to Match Full-Scale Wing Ice Accretion

Sudhindra Uppuluri and Michael S. Selig
Department of Aeronautical and Astronautical Engineering
University of Illinois at Urbana–Champaign
Urbana, Illinois 61801

40th AIAA Aerospace Sciences Meeting and Exhibit
January 14-17, 2002/Reno, NV

Hybrid Wing Design to Match Full-Scale Wing Ice Accretion

Sudhindra Uppuluri* and Michael S. Selig†
Department of Aeronautical and Astronautical Engineering
University of Illinois at Urbana–Champaign
Urbana, Illinois 61801

A hybrid wing design methodology has been formulated to provide guidance in designing hybrid wings that simulate the droplet impingement and ice accretion of full-scale wings. The hybrid wing in this context has a smaller chord than the full-scale wing and hence can be easily tested in the existing icing tunnels which are too small to perform ice accretion testing of full-scale commercial aircraft wings. This paper presents a systematic study to design hybrid wings based on the hybrid airfoil design methodology that has been previously developed and validated by Saeed et al. The new wing design methodology involves understanding the effect of various factors causing three dimensionality in the flow such as induced effect and spanwise flow on ice accretion. Three wing configurations with increasing three-dimensionality in the flow were analyzed at various angles of attack. The ice accretions on the full-scale and hybrid wings were compared, and the hybrid wing was modified, if necessary, using aerodynamic twist or flap to match the leading edge flowfield and hence ice accretion of the full-scale wing.

Nomenclature

AR	aspect ratio of the wing
c	airfoil chord
C_d	airfoil drag coefficient
C_D	wing drag coefficient
C_l	airfoil lift coefficient
C_L	wing lift coefficient
F_r	Froude number, $V_\infty/\sqrt{cg}$
K	droplet inertia parameter, $\rho_w \delta^2 V_\infty / 18 c \mu$
LWC	liquid water content
M	freestream Mach number
n	transition amplification factor
Re	Reynolds number based on full-scale airfoil chord
R_u	droplet freestream Reynolds number, $\rho \delta V_\infty / \mu$
α	angle of attack, deg
α_{des}	design angle of attack for a hybrid airfoil, deg
β	local impingement efficiency
δ	droplet diameter
δ_f	flap deflection
μ	air viscosity

*Graduate Research Assistant, Department of Aeronautical and Astronautical Engineering. Currently: Technical Specialist, Flowmaster USA, Inc., e-mail: sudhi@fmusa.com. Student Member AIAA.

†Associate Professor, 306 Talbot Laboratory, 104 S. Wright St. e-mail: m-selig@uiuc.edu. Senior Member AIAA.

Introduction

It has been long known that ice formation on aircraft wings has adverse effects on aerodynamics and poses a major threat to aircraft safety.[1,2] The adverse effects of ice accretion are mainly due to the gross change in the cross-sectional geometry of the wing with accumulated ice. The determination of the critical ice accretion and its aerodynamic effect on a set of modern airfoils, typically of those in use on aircraft, is underway at NASA Glenn Research Center. The research reported here is part of this larger effort.

Ice accretion testing of full-scale wings in existing icing tunnels has been limited due to uncertainties in ice accretion scaling.[3] One way to expand the usefulness of existing tunnels is to test hybrid airfoils and potentially wings. The hybrid airfoil[4–7] is one that retains the full-scale airfoil leading edge, but has a shortened aft section and thereby a shorter overall chord. When suitably designed using existing computational techniques, the hybrid airfoil can be tested at full-scale conditions to produce full-scale ice accretions and in doing so bypass the issue of ice accretion scaling. A key advantage is that full-scale ice accretions can be obtained on smaller models in smaller tunnels at a fraction of the costs of full-scale wind tunnel testing. While this technique has worked well for the two-dimensional case, the question remains how applicable are these ideas to three-dimensional testing of wings.

This paper presents a methodology to design hybrid wings based on the hybrid airfoil design methodology. The hybrid wing design methodology involves understanding various factors causing three-dimensionality in a flow and modifying the hybrid wing to match the ice accretion of the full-scale wing.

Computational Tools

The following tools have been extensively used in the design and analysis of the full-scale and hybrid airfoils used in this study.

PROFOIL[8,9] is a multipoint inverse airfoil design code based on conformal mapping in which the airfoil is generated from a circle that is mapped to an airfoil. The design of an airfoil is achieved by specifying a velocity distribution. The velocity distribution, which is not completely arbitrary, is governed by continuity and closure constraints that form an integral part of the inverse design methodology. A unique feature of the approach, apart from its multipoint design capability is that the airfoils can be designed to satisfy certain additional desired parameters such as a net pressure recovery, airfoil thickness, trailing-edge thickness, pitching moment, etc. Then a multi-dimensional Newton iteration scheme is employed to iterate on the available free variables to satisfy the design criteria.

XFOIL[10] is a code for viscous/inviscid analysis and direct or mixed-inverse design of subcritical airfoils. The inviscid analysis is performed using a linear-vorticity panel method with a Karman-Tsien compressibility correction. The viscous displacement effects are accounted for by superimposing source distributions on the airfoil and wake, based on a displacement thickness predicted by an integral boundary layer method. Both laminar and turbulent layers are treated in the formulation, with an e^n-type transition prediction method. A value of $n = 9$ was used in all of the cases in this study. The boundary layer equations are solved simultaneously with the inviscid flowfield by a global Newton iteration method that makes it a very suitable tool for rapid airfoil analysis.

AIRDROP[11,12] is an airfoil water-droplet impingement code that predicts droplet trajectories and the resultant impingement efficiency on single-element airfoils in incompressible flow. The code has been validated against NACA airfoil droplet impingement data and compares well when the cloud droplet size distribution is modeled correctly and the code is run matching the airfoil lift coefficient.

The numerical procedure employed by AIRDROP consists of two steps. First, the flowfield around the airfoil is determined by Woan's method, which is based on Theodoreson's conformal mapping method. Second, single water droplet trajectories are calculated from the trajectory equation, which in non-dimensional form contains the similarity parameters R_u, F_r and K. Based on the size of the droplets under consideration, the effect of gravity on the droplets is negligible and, therefore, F_r is ignored. Thus, given R_u, K, the droplet initial conditions, and the airfoil geometry, single water droplet trajectories are determined from the trajectory equation. The individual droplet trajectories are combined to calculate the local impingement efficiency $\beta\,(= dy_o/ds)$.

HYBRID is an integrated code developed by Saeed et al.[4–7] for hybrid airfoil design. It integrates PROFOIL for the aft section design. The flowfield analysis is based on the EPPLER[13] panel method code; whereas, the droplet impingement analysis is based on AIRDROP. The HYBRID code takes the 'nose' section from the full-scale airfoil (determined by the droplet impingement limits on the full-scale airfoil) and designs an aft section for this 'nose' such that the collection efficiency distribution β of the hybrid airfoil agrees closely with that of the full-scale airfoil. PROFOIL is used to control the design lift coefficient for the given design angle of attack as well as the geometric details involving the connection between the aft section and the full-scale leading edge. It has been shown that having nearly the same amount of circulation for the full-scale and hybrid airfoils causes similar leading-edge flow and hence similar droplet impingement on the full-scale and hybrid airfoils.

The final step of the hybrid airfoil design uses a modified version of XFOIL, called here for the sake of discussion XDROP. This modified version of XFOIL was obtained by integrating the droplet trajectory and impingement code from AIRDROP into the XFOIL code. This modification was done to take advantage of XFOIL's capability of handling viscous effects unlike the AIRDROP code, which is based on inviscid flow. The addition of droplet-trajectory and impingement-characteristics calculation subroutines in XFOIL not only resulted in its enhanced capability as a powerful airfoil design and analysis tool but also resulted in substantial savings in computational effort and time to accomplish a hybrid airfoil design.

The three-dimensional ice accretion simulation process used for this study was performed using LEWICE3D and can be broadly divided into a six step process as shown in the Fig. 1. The details of ice accretion simulation procedure with LEWICE3D is now described.

PMARC[14–16] is a three-dimensional low-order potential flow panel method code. It calculates the inviscid potential flow solution over three-dimensional surfaces. The whole surface is discretized into small quadrilateral regions called 'panels.' A constant doublet and source distribution is assumed at every panel. The formulation used in PMARC provides a second-order accurate solution. The code can handle very large problems (around 10,000 panels) and can be used for external or internal flow computations.

The ICEGRID program[17] was specifically developed to generate a three-dimensional wing grid that is optimized for droplet trajectory calculations. The grid is used to discretize the flowfield around the wing. The ICEGRID program also produces the minimum number of grid points that reduces the panel code calculation time. The code requires two input files: one containing the surface geometry information (obtained

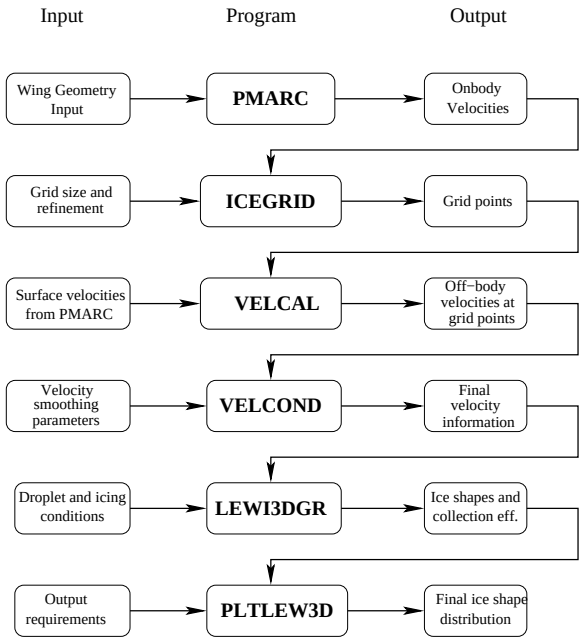

Fig. 1 Flowchart of the wing ice iccretion analysis procedure.

from PMARC) and the second containing the information of the grid size, grid orientation, and various refinement functions. The refinement functions could include point refinement, line refinement, local part refinement or a combination of above. The code, like an oct-tree method, recursively divides the original grid volume until gthe refinement criteria for each cell has been met.

The VELCAL program calculates velocities at each of the grid points. This program uses the flow solution stored by PMARC to generate the velocities on the grid.

The VELCOND program uses a surface velocity interpolation technique to smooth off-body velocities generated by the panel code PMARC.

The LEWICE3D program[17,18] (in software named LEWI3DGR) simulates droplet impingement on the wing and calculates collection efficiency and ice shapes on three-dimensional external surfaces. A higher-order Runge-Kutta integration scheme is used to calculate the arbitrary streamlines. An Adams-type predictor-corrector trajectory integrated scheme has been implemented to calculate arbitrary trajectories. Schemes for calculating tangent trajectories, collection efficiencies and concentration factor for arbitrary regions of interest for single droplets and droplet distributions have been incorporated. From the input flowfield, the LEWICE3D program calculates the surface streamlines, droplet run-back along these surface streamlines and partial freezing of the run-back droplets to form the ice shape. A heat transfer program is used to calculate the freezing of the droplets and formation of the ice shape. This code is based on the NASA Glenn two-dimensional ice accretion code LEWICE[19,20] and was developed at the NASA Glenn Research Center (formerly NASA Lewis.)

The PLTLEW3D is a post-processing program that manipulates the output files generated from the LEWICE3D program and generates the desired plots of the key variables of the ice accretion process such as collection efficiency, ice shapes, freezing fraction and heat transfer coefficients among others. Various flags can be set in the configuration file for the PLTLEW3D program to obtain the desired type of plots.

Details of Computational Procedure

A dimensional chord of 40 in. for the full-scale wing and 20 in. for the hybrid wing was assumed (the hybrid airfoil is 50% chord of the full-scale). The number of panels for all of the PMARC wing geometries was around 5000. The panels were concentrated near the leading edge where the ice accretion occurs to generate good resolution of the surface velocity distribution and ice shape. Non-standard values for the PMARC parameters RFF = 30, RCORES = 0.002 and RCOREW = 0.002 were used for off-body velocity calculations. The large value of RFF was used taking into account the small size of the panel near the leading edge. The small values of RCORES and RCOREW were used to bypass the singularity fix in the PMARC program.[17] The singularities were handled using a better interpolation scheme in the VELCOND program.

To discretize the flowfield, three different refinement functions were input into the ICEGRID program. The maximum cell size of 16 in. was used in x, y and z directions. The idea behind using the refinement functions is to have a high resolution of grid points where the droplet trajectories meet the wing. Care was taken so that the panel spacing for the PMARC model was fine where there was a fine grid. A minimum cell size of 0.05 in. was used near the leading edge for all the grids generated in this study. Good refinement of the grid points and the surface panels led to accurate ice accretion results with minimal computation time.

As mentioned, the off-body velocities were generated using the program VELCAL. Calculation of off-body velocities is fairly computationally intensive. A typical single run in this study took around 10–15 hrs and was usually done using overnight batch runs. The off-body velocities generated from the VELCAL program were input into the LEWICE3D program for ice accretion calculations. A user-input file for the LEWICE3D program was generated such that approximately 400 trajectories were calculated at each wing section of interest. A typical LEWICE3D run to calculate the droplet impingement, heat transfer and ice accretion data for the four sections was relatively quick and generally took less than 3 min. of CPU time on a Pentium-III 600-MHz PC.

Hybrid Wing Design Methodology

The hybrid wing design methodology was formulated to provide guidance in designing hybrid wings that simulate droplet impingement and ice accretion of larger full-scale wings. This methodology is primarily valid for incompressible, inviscid flow though it can be used, in certain circumstances, to design hybrid wings in viscous flow when the viscous effects are not too large (i.e., when there is limited separated flow). This methodology is an extension of the hybrid airfoil design methodology developed by Saeed et al.[4–7]

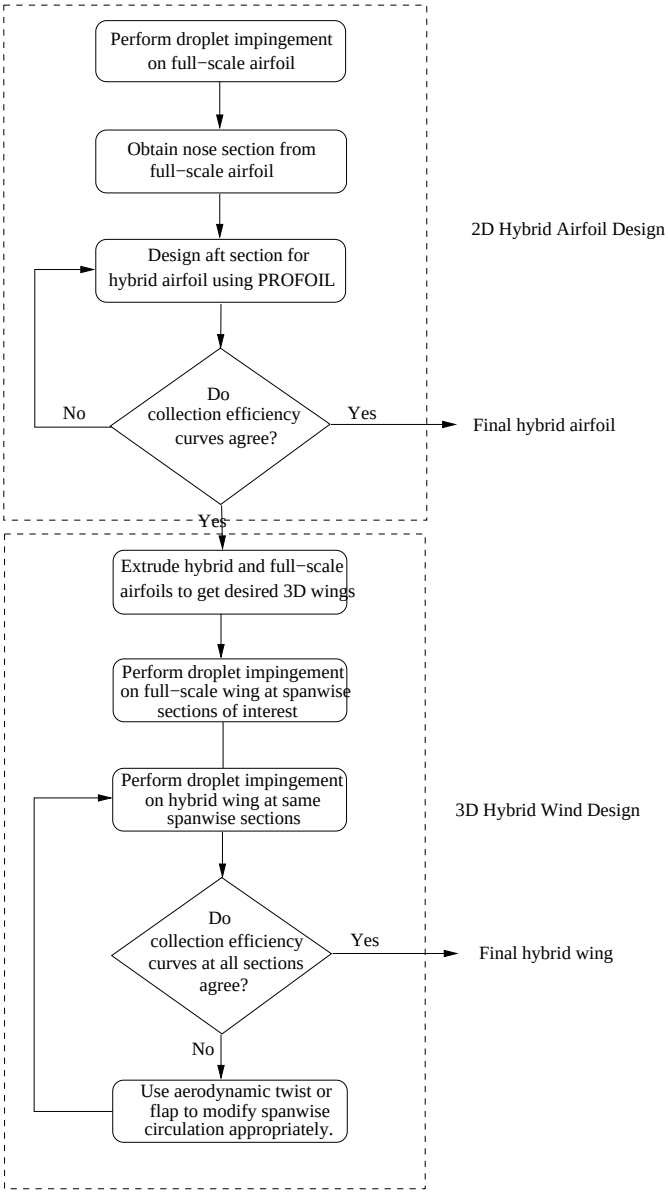

Fig. 2 Hybrid wing design procedure.

Figure 2 outlines the hybrid wing design methodology. First, an initial geometry of the sub-scale (say 50%) chord hybrid airfoil was obtained using the program HYBRID. Since the hybrid airfoil has 50% chord, the cC_l vs. α curve slope for the hybrid airfoil will be half that for the 100%-chord airfoil (see Fig. 3). The angle of attack at which the hybrid airfoil is designed to have the same droplet impingement distribution as the full-scale airfoil is the design angle of attack α_{des}. At this design point α_{des}, the hybrid airfoil and the full-scale airfoil have nearly the same circulation and hence similar droplet impingement. It can seen in the Fig. 3 that the hybrid airfoil has slightly less circulation than the full-scale airfoil at the design angle of attack. It has been shown in the study done by Saeed et al.[6,7] that the hybrid airfoil requires around 4.5% less circulation than the full-scale to simulate full-scale droplet impingement characteristics. A lower value of overall circulation for the hybrid airfoil can be attributed to the distribution of vorticity which for the hybrid airfoil is more concentrated near the leading edge resulting in a greater local upwash in close proximity to the airfoil.

If, in the preliminary design (the first iteration) of the hybrid airfoil, the desired β-curve distribution is not achieved, the aft section of the hybrid airfoil is redesigned by changing the appropriate input parameters to HYBRID accordingly. The agreement in the β-curve of the full-scale and hybrid airfoils is determined by how well the impingement limits, peak droplet impingement, and the distribution agree. No mathematical closeness criteria is used. Once the β-curve of the full-scale and hybrid airfoils agree well, the hybrid airfoil viscous performance and droplet impingement characteristics were analyzed using XDROP at the appropriate Reynolds numbers. The hybrid airfoil was iterated again, if necessary, until a good agreement in the β-curve of the full-scale and hybrid airfoils was achieved.

A preliminary hybrid wing was then generated by extruding the hybrid airfoil into the required three-dimensional shape—the hybrid wing. For example, a 26-in. straight extrusion of the hybrid airfoil with a chord of 10 in. will generate a wing with $AR = 2.6$. The ice accretion computations were then performed on the full-scale and hybrid wings. The full-scale and hybrid wings were analyzed under similar flow and icing conditions and the ice formations were compared at various spanwise locations. To first order at a particular station, any ice accretion difference that may exist between the hybrid and full-scale wings is a result of there being a difference in the local inflow, which is driven by both the downwash and local cCl. This situation is most likely to occur near the tips of the hybrid and full-scale wings. If the ice accretions on the full-scale and hybrid wings differ significantly, the spanwise sectional lift distribution for hybrid wing is adjusted using either aerodynamic twist or a flap near the tip of the hybrid wing such that the lift distribution and hence the ice accretions for the full-scale and hybrid wings agree at all sections. The amount of twist or flap deflection is determined by conducting a

parametric study for varying twists or flap deflection and their effect on sectional lift distribution cC_l of the wing.

Case Study

The full-scale airfoil considered in this study was the NACA 64-008A airfoil. Three different hybrid airfoils for design points of α_{des} of 0, 4 and 8 deg were designed using the two-dimensional hybrid airfoil design methodology. The full-scale and hybrid airfoils are shown in Fig. 4.

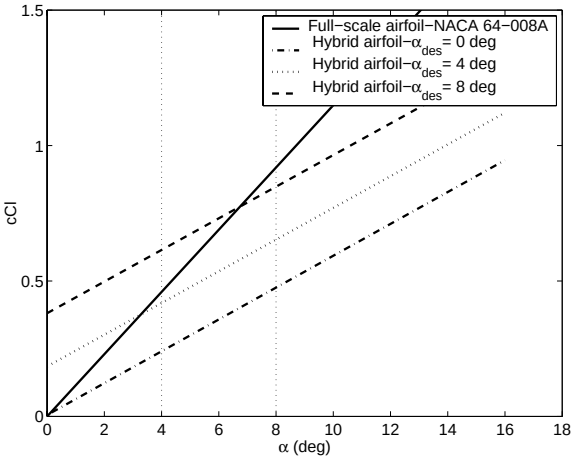

Fig. 3 Two-dimensional lift curve comparison for full-scale and hybrid airfoils.

As discussed earlier, these individual hybrid airfoils approximately match the circulation of the full-scale airfoil at the design angle of attack α_{des}. Figure 3 shows the two-dimensional lift curves of the full-scale and hybrid airfoils. The β-curves for the full-scale and three hybrid airfoils with α_{des} of 0, 4 and 8 deg showed good agreement at α of 0, 4 and 8 deg respectively.[21]

In order to study the effect of three dimensionality in the flow on ice accretion and to test the validity of using the existing hybrid airfoil design methodology to design hybrid wings, the following three wing configurations were chosen: straight wing with AR of 7, straight wing with AR of 2.6 and swept wing with AR of 2.6 as shown in Fig. 5. These configurations have increasing three dimensionality in flow and make good candidates for studying the effect of three dimensionality in the flow on the ice accretions. Ice accretions at four spanwise sections (specifically, 20%, 40%, 60% and 80% semi-span stations) on these configurations were studied for the full-scale wing and the hybrid wing.

A single icing condition was chosen for the study to typify the icing condition on a commercial transport airplane. The icing condition for the analyses presented in this study was: airspeed of 135 m/s, static temperature of 262 K, icing time of 1800 sec, liquid water content (LWC) of 0.51 g/m^3, and median volume diameter (δ) of 20 μm. All of the computations

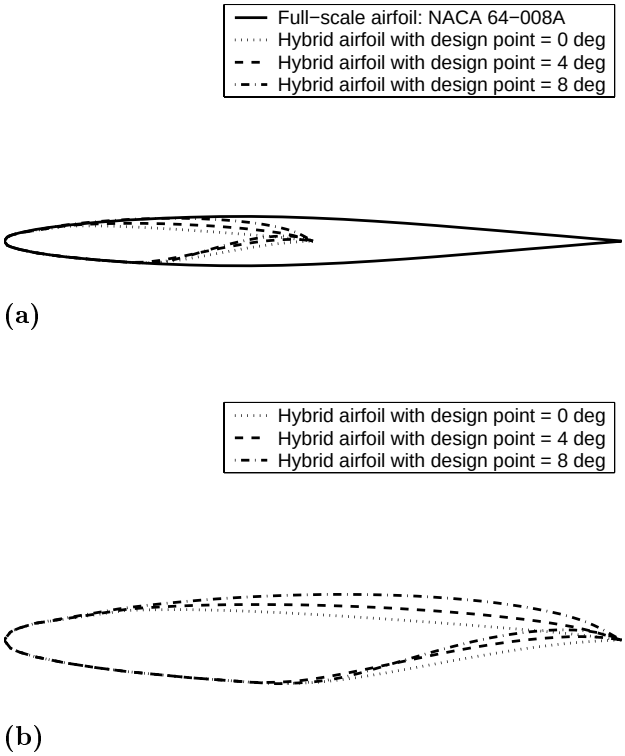

Fig. 4 Full-scale NACA 64-008A airfoil and hybrid airfoils at α_{des} of 0, 4, and 8 deg shown together (a) and with enlarged hybrid airfoils separate (b).

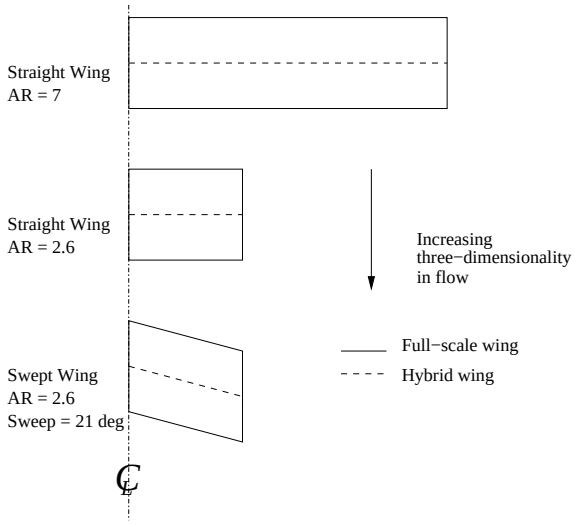

Fig. 5 Top view of configurations of wings studied.

presented here were performed on a Pentium-III 600-MHz PC. The ice accretion calculations on the three configurations of wings at α of 0, 4 and 8 deg were performed using the computational procedure described in the previous sections. A single grid was used for the whole wing in all the cases except for the wing with $AR = 7$ case. For the $AR = 7$ case, the wing was dimensionally fairly large ($b/2 = 140$ in.). Generating a fine grid for the whole wing is computationally intensive and was unnecessary since there is a little spanwise flow and a grid of $\pm$ 10 in. of the section of interest is good enough to capture the droplet trajectories. Thus, for the $AR = 7$ case, four separate grids of 20-in. width were generated at the four sections of interest to minimize computational time.

The results presented in this paper are for the straight wing configuration with AR of 7. Results for the other wings can be found in Ref. 21. Figure 6 below shows the various sections of interest. Figures 7 and show collection efficiency distribution and ice accretion obtained from the LEWICE3D calculations.

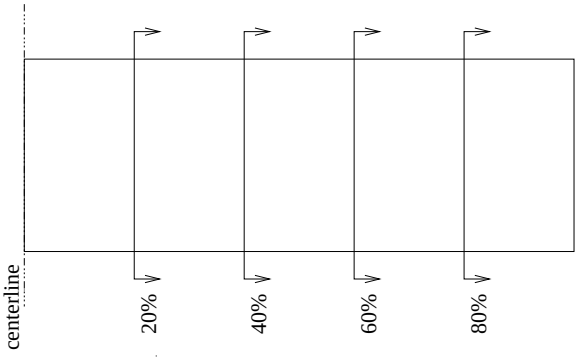

Fig. 6 Schematic of the four spanwise sections on the wing with AR of 7.

It can be seen from Figs. 7 and that the ice shapes and β-curves for the full-scale and hybrid wings agree closely for straight wing configuration with an aspect ratio of 7 at angles of attack of 0, 4 and 8 deg without any modifications for spanwise lift to the hybrid wing. Similar good agreement in collection efficiency and ice shapes without modifications were observed for the straight wing with $AR = 2.6$ and the swept wing with $AR = 2.6$. It is surprising that for wing configurations with high three-dimensional flow (e.g., swept wing with AR of 2.6 at α of 8 deg) the β-curves and hence the ice shapes on the full-scale and the hybrid wing agree fairly closely.

In order to understand the physical phenomena behind this good agreement, the lift curves (cC_l vs. α) were plotted for the two-dimensional and three-dimensional cases for the full-scale and hybrid wings. Figures 9, 10 and 11 show the comparison of lift curves for the straight wing with $AR = 2.6$ configuration at $\alpha = 0$, 4 and 8 deg respectively. It is seen that, at a given design angle of attack α_{des}, the full-scale and

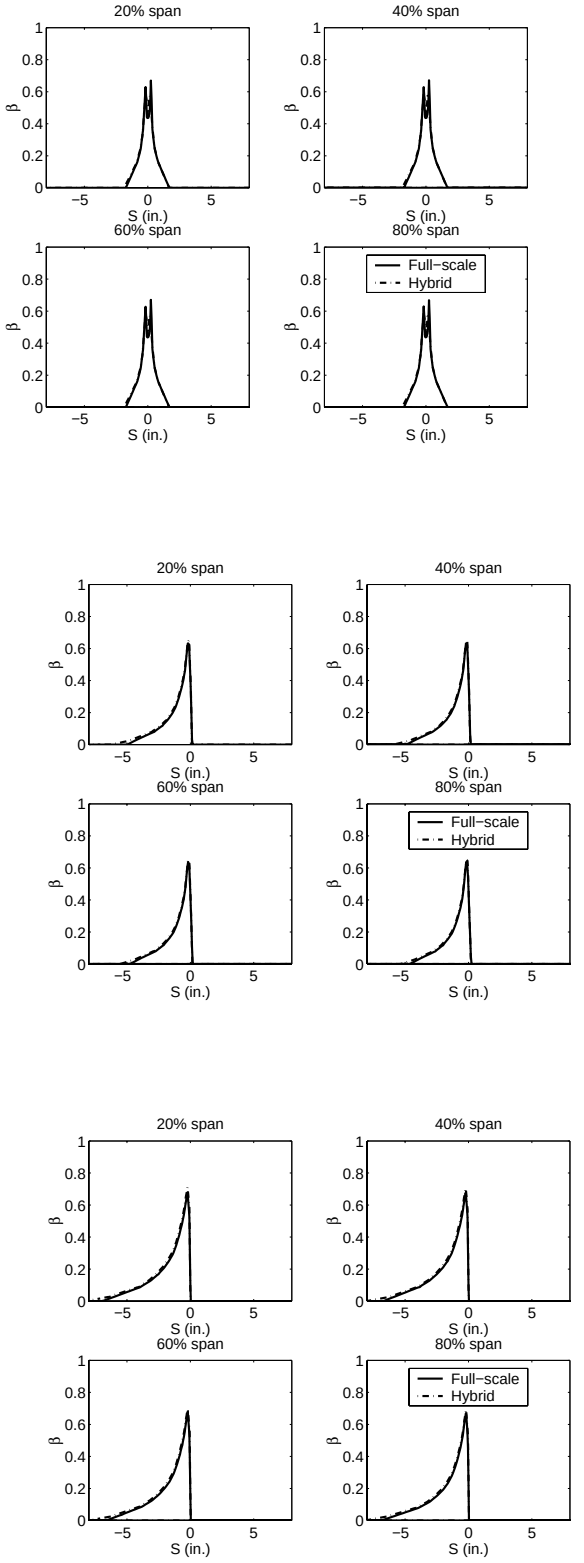

Fig. 7 Collection efficiency β comparison at the four spanwise stations on the wing with AR of 7 at angles of attack of (a) 0 deg, (b) 4 deg, and (c) 8 deg.

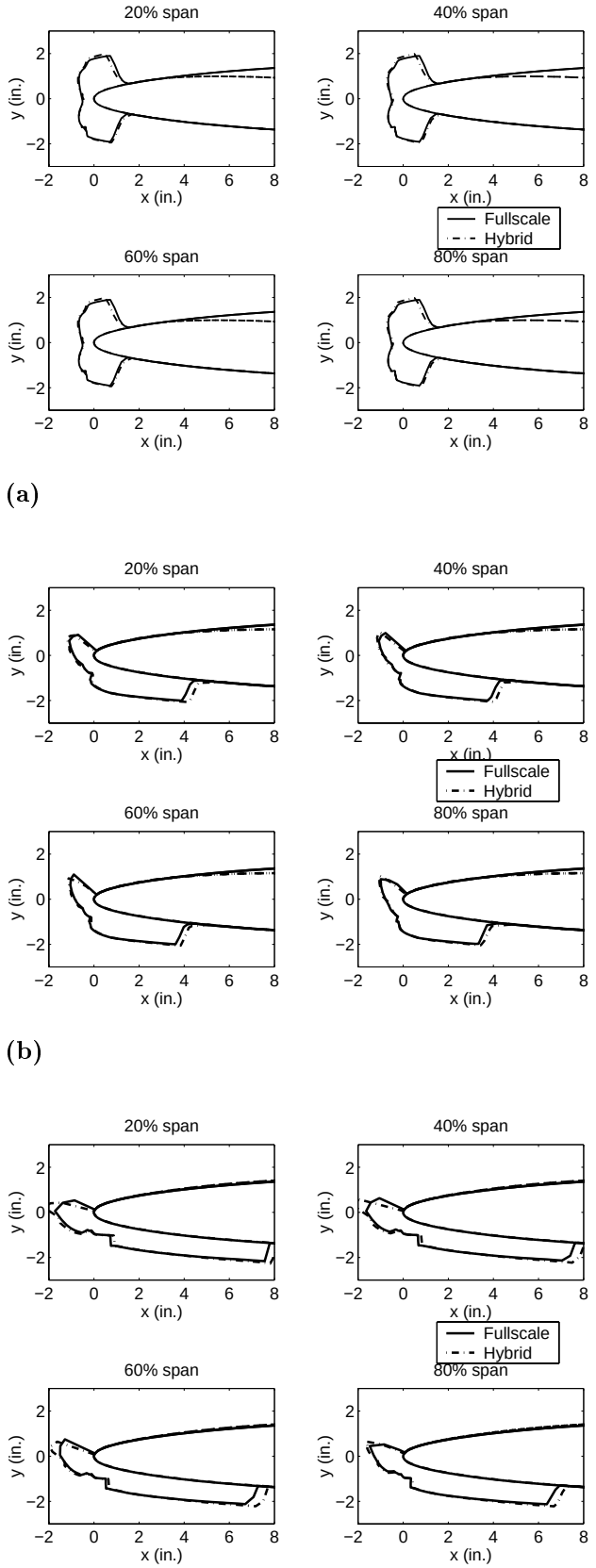

Fig. 8 Ice shape comparison at the four spanwise sections on the wing with AR of 7 at angles of attack of (a) 0 deg, (b) 4 deg, and (c) 8 deg.

hybrid airfoils were designed to have nearly the same circulation and therefore have similar droplet impingement curves. However, it is noted that the full-scale and hybrid wings also have nearly the same lift at the design angle of attack α_{des} causing similar droplet impingement and hence similar ice shapes.

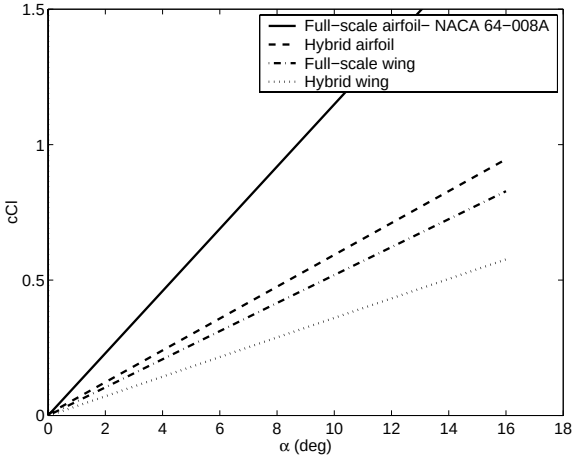

Fig. 9 2D and 3D lift curves for full-scale and hybrid wings at $\alpha = 0$ deg; 20% span section; straight wing with $AR = 7$.

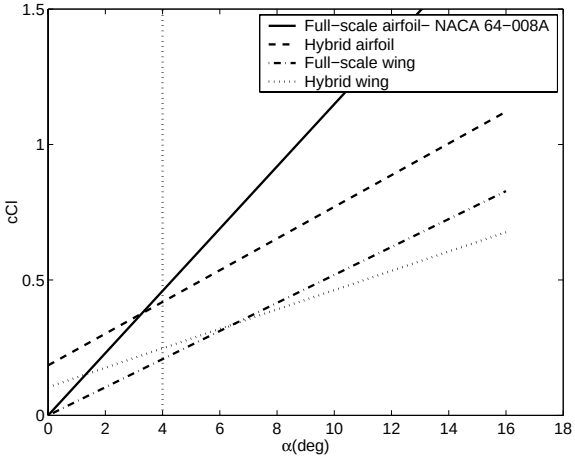

Fig. 10 2D and 3D lift curves for full-scale and hybrid wings at $\alpha = 4$ deg; 20% span section; straight wing with $AR = 7$.

It can be seen that although the lift curve slopes for the wings change due to induced effect the local cC_l (and hence circulation) for the full-scale wing is approximately the same as that for the hybrid wing at all the sections at a given design angle of attack α_{des}. It can also be noted that the lift curve slope drop for the full-scale airfoil to the full-scale wing is larger than that for the hybrid wing. This larger drop is because the hybrid airfoil has 50% chord of the full-scale airfoil and hence, for a given semi-span of the wing, the aspect ratio of the hybrid wing is twice that of the full-scale wing. Thus, the hybrid wing will have

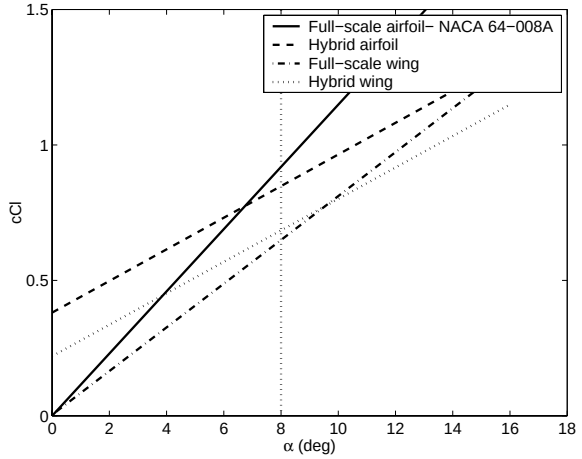

Fig. 11 2D and 3D lift curves for full-scale and hybrid wings at $\alpha = 8$ deg; 20% span section; straight wing with $AR = 7$.

less induced effect than the full-scale wing. Though the induced effect causes a different change in the lift curve slopes for the full-scale and hybrid wings, the cC_l (and hence circulation) of the full-scale and the hybrid wing at a given design angle of attack α_{des}, remains approximately the same and hence they have the same ice accretion at that angle of attack.

A closer look, however, reveals a slight disagreement in the ice shapes and collection efficiency at the outboard section (see Fig.). This disagreement is mainly due to a high induced effect that causes a difference in sectional lift. Figures 12, 13 and 14 show the comparison of spanwise cC_l distribution for the three configurations at angles of attack of 0, 4 and 8 deg.

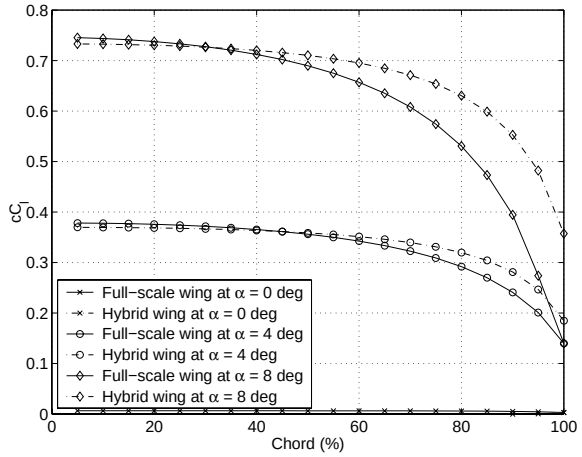

Fig. 12 Spanwise cC_l distribution for the full-scale and hybrid wings at $\alpha = 0$, 4 and 8 deg; straight wing with AR of 7.

It can be noted that there is a difference in spanwise circulation towards the tip of the wing, which causes disagreement in the ice shapes for the full-scale and hybrid wings. Though a spanwise circulation correction method such as flap towards the outboard section

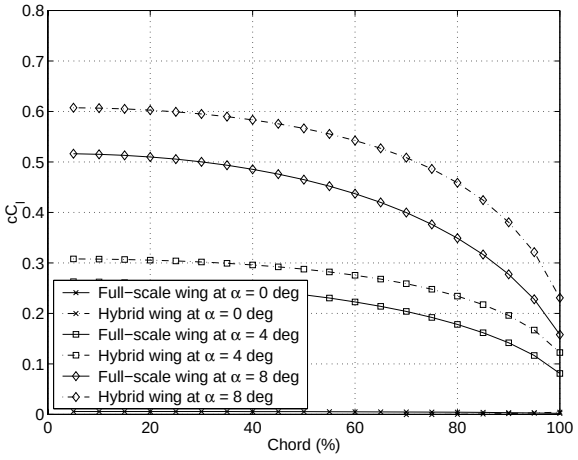

Fig. 13 Spanwise cC_l distribution for the full-scale and hybrid wings: $\alpha = 0$, 4 and 8 deg; straight wing with AR of 2.6.

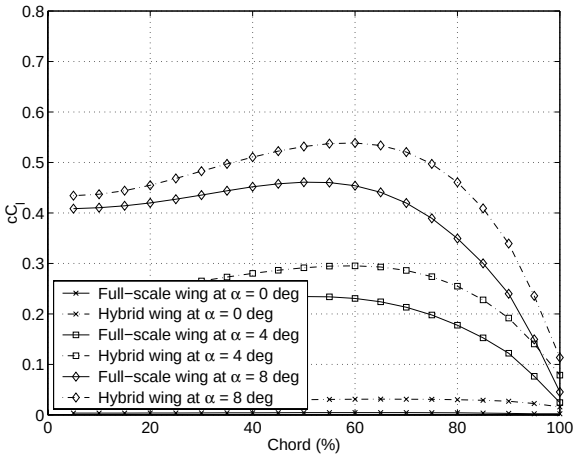

Fig. 14 Spanwise cC_l distribution for the full-scale and hybrid wings at $\alpha = 0$, 4 and 8 deg; swept wing with AR of 2.6.

can be used to obtain a better match of sectional lifts and hence ice shapes, it is undesirable. The ice accretions at the outboard section for the full-scale and hybrid wing (see Fig.) are within an acceptable range and can be considered a fairly good match. The decision is purely based on the designer's experience and judgement. No numerical closeness criteria is used to decide the degree of agreement in the ice shapes. A more thorough understanding of this tip effect would require wind tunnel testing.

Conclusions

A systematic study of ice accretions was conducted on full-scale and hybrid wings with increasing three-dimensionality in flow. It was found that there is a fairly good agreement in ice shapes for the full-scale and hybrid wings for all of the configurations studied and at all angles of attack considered. At higher angles of attack and for wing configurations with highly

three-dimensional flows (straight wing with $AR = 2.6$ and swept wing with $AR = 2.6$), however, there is a slight disagreement in the ice shapes at the outboard sections. This disagreement in ice shapes is due to the difference in sectional lift for the full-scale and hybrid wings at the outboard sections. Good agreement in circulation will achieve a close agreement in ice shapes for the full-scale and hybrid wings. A spanwise circulation correction method such as flap towards the outboard section or an aerodynamic twist can be used to adjust the sectional lift of the hybrid wing in order to obtain a better match of ice shapes.

There was a good agreement in ice shapes for the full-scale and hybrid wings for all wing configurations and angles of attack considered in this study. Thus, a hybrid wing can be designed for a given design angle of attack α_{des} using a hybrid airfoil designed at the same angle of attack α_{des}. This fact greatly simplifies the design of a hybrid wing for full-scale leading-edge ice accretion testing. It should be kept in mind that the flowfield calculations were done using PMARC, which predicts potential flow. PMARC will fail to predict with sufficient accuracy flows with separation. Therefore, the hybrid wing design methodology presented in this paper should be used with caution for cases where there will be separation on the full-scale wing.

Acknowledgments

This research was sponsored by NASA Glenn Research Center under the grant NASA NCC 3-509. We would like to thank the grant monitor Harold (Gene) Addy of NASA Glenn Research Center for his helpful direction during the course of this work. Also, guidance from Dr. Farooq Saeed on hybrid airfoil design, from Prof. Michael Bragg on using AIRDROP and from Colin Bidwell on LEWICE3D is gratefully acknowledged.

References

[1]Bron, R., "Icing Problems and Recommended Solutions," AGARDograph 16, November 1957.

[2]Perkins, P. and Rieke, W., "Aircraft Icing Problems - After 50 years," *AIAA Paper*, , No. 93, 1993.

[3]Anon., "Selected Bibliography of NACA-NASA Aircraft Icing Publications," NASA TM 81651, August 1981.

[4]Saeed, F., Selig, M., and Bragg, M., "Design of Subscale Airfoils with Full-Scale Leading-Edges for Ice Accretion Testing," *Journal of Aircraft*, Vol. 34, No. 1, 1997, pp. 94–100.

[5]Saeed, F., Selig, M., and Bragg, M., "Hybrid Airfoil Design Method to Simulate Full-Scale Ice Accretion Throughout a Given α-Range," *Journal of Aircraft*, Vol. 35, No. 2, 1998, pp. 233–239.

[6]Saeed, F., Selig, M., and Bragg, M., "Hybrid Airfoil Design Procedure Validation for Full-Scale Ice Accretion Simulation," *Journal of Aircraft*, Vol. 36, No. 5, 1999, pp. 769–776.

[7]Saeed, F., *Hybrid Airfoil Design Methods for Full-scale Ice Accretion Simulation*, Ph.D Dissertation, University of Illinois at Urbana–Champaign, Urbana, IL, January 1999.

[8]Selig, M. S. and Maughmer, M. D., "A Multi-Point Inverse Airfoil Design Method Based on Conformal Mapping," *AIAA Journal*, Vol. 30, No. 5, May 1992, pp. 1162–1170.

[9]Selig, M. S. and Maughmer, M. D., "Generalized Multipoint Inverse Airfoil Design," *AIAA Journal*, Vol. 30, No. 11, November 1992, pp. 2618–2625.

[10]Drela, M., "XFOIL: An Analysis and DesignSystem for Low Reynolds Number Airfoils," Vol. 54 of *Lecture Notes in Engineering: Low Reynolds Number Aerodynamics*, Springer-Verlag, June 1989.

[11]Bragg, M. B., *AIRDROP: Airfoil Droplet Impingement Code*, University of Illinois at Urbana–Champaign, Urbana, IL, To be published as a NASA CR.

[12]Bragg, M. B., *Rime Ice Accretion and Its Effect on Airfoil Performance* , Ohio State University, Columbus, OH, Ph.D Dissertation, 1981.

[13]Eppler, R. and Somers, D., "A Computer Program for the Design and Analysis of Low-Speed Airfoils," NASA TM 80210, August 1980.

[14]Pinella, D. and Garrison, P., *CMARC, Three-Dimensional Low Order Panel Method Code, Version 2.1*.

[15]Ashby, D., Dudley, M., and Iguchi, S., "Development and Validation of an Advanced Low-Order Panel Method," NASA TM 1011024, October 1998.

[16]Maskew, B., "Program VSAERO Theory Document: A Computer Program for Calculating Nonlinear Aerodynamic Characteristics of Arbitrary Configurations," NASA CR 4023, September 1987.

[17]Bidwell, C., Pinella, D., and Garrison, P., "Ice Accretion Calculations for a Commercial Transport using LEWICE3D, ICEGRID3D and CMARC Programs," NASA TM 208895, January 1999.

[18]Bidwell, C. and Potapczuk, M., "Users Manual for the NASA Lewis Three-Dimensional Ice Accretion Code (LEWICE3D)," NASA TM 105974, December 1993.

[19]Wright, W., "A Summary of Validation Results for LEWICE 2.0," NASA CR 208687, November 1998.

[20]Wright, W., "User Manual for the NASA Glenn Ice Accretion Code LEWICE Version 2.0," NASA CR 209409, September 1999.

[21]Uppuluri, S., *Hybrid Wing Design to Simulate Full-scale Ice Accretion* , University of Illinois at Urbana–Champaign, Urbana, IL, M.S Thesis, 2001.